Modeling orientational randomization in zeolites: A new probe of intracage mobility, diffusion and cation disorder

Scott M. Auerbach[a)]
Departments of Chemistry and Chemical Engineering, University of Massachusetts, Amherst, Massachusetts 01003

Horia I. Metiu
Departments of Chemistry and Physics, University of California, Santa Barbara, California 93106

(Received 16 September 1996; accepted 14 November 1996)

We have performed kinetic Monte Carlo simulations of benzene orientational randomization (BOR) and diffusion in Na-Y zeolite for various Na(II) occupancies and Na(II) spatial patterns. Full Na(II) occupancy gives BOR rates controlled by intracage motion, whereas half Na(II) occupancy gives BOR rates sensitive to both intracage and intercage motion, but insensitive to particular Na(II) spatial patterns. Alternatively, BOR with one quarter Na(II) occupancy demonstrates *qualitative sensitivity* to different Na(II) spatial patterns. Calculated diffusion coefficients vary weakly with decreasing Na(II) occupancy until ca. one Na(II) per supercage. Diffusion coefficients and mean square displacements reveal no information about intracage motion, and are insensitive to different spatial patterns of Na(II) cations. Our computational results thus suggest that measuring orientational randomization in zeolites can provide important information regarding intracage motion, diffusion and cation disorder.
[S0021-9606(97)51007-5]

I. INTRODUCTION

The transport properties of adsorbed molecules[1] play a central role in catalytic and separation processes[2] that take place within zeolite cavities.[3] Although significant effort has been devoted to understanding diffusion in zeolites,[1] several fundamental questions persist: What causes discrepancies between diffusion coefficients measured by different techniques? What structural aspects of zeolites can be probed by diffusion measurements? How can structural details be revealed if diffusion measurements are insensitive to them? Below we begin to answer these questions using kinetic modeling techniques applied to benzene in Na-Y zeolite. Our computational results suggest that measuring benzene orientational randomization in Na-Y can provide important information complementary to that obtained from diffusion measurements.

In a recent series of theoretical studies, we have explored how fundamental intracage and intercage jumps control benzene mobility in Na-X (Si:Al=1.0) and Na-Y (Si:Al=2.0).[4–6] Our calculations indicate that activation energies from long length scale diffusion measurements, e.g., pulsed field gradient NMR,[1,7] should be interpreted as site-to-window activation energies. Moreover, we suggest that results from NMR relaxation experiments for benzene in a series of faujasites,[8–11] while reported as diffusion coefficients, should be interpreted as time scales for *intracage* orientational randomization, and hence should not agree with pulsed field gradient NMR results. In an effort to model NMR relaxation data as closely as possible, which may complement diffusion data, we use kinetic Monte Carlo[4,6,12–14] to calculate the orientational correlation function accounting for randomization of benzene's six-fold axis. The results presented below clearly indicate that NMR correlation times for benzene in Na-Y with full Na(II) occupancy are indeed controlled by intracage hopping processes.

An important parameter characterizing the electrostatic environment of a zeolite is the Si:Al composition ratio, which ranges between one and infinity in different systems, and which varies inversely with the density of exchangeable cations in the solid.[3] Molecular mobilities in zeolites tend to increase with an increasing Si:Al ratio, especially for nucleophilic adsorbates which become trapped with long residence times at cationic sites. To deepen our understanding of this trend, we use kinetic Monte Carlo to calculate orientational correlation functions and mean square displacements for benzene in Na-Y (Si:Al$\geqslant$2.0), to determine how decreasing Na(II) cation occupancy affects orientational randomization rates and diffusion coefficients. The results presented below indicate that calculated diffusion coefficients vary weakly with decreasing Na(II) occupancy until *ca*. one Na(II) per supercage, and that mean square displacements reveal no information about intracage motion or spatial patterns of Na(II) cations. Alternatively, we predict that cation vacancies cause non-exponential decay of the orientational correlation function, providing important information regarding intracage motion, diffusion and cation disorder.

The remainder of this paper is organized as follows: in Sec. II we discuss the relevant orientational correlation function and relate it to various NMR measurements of reorientation dynamics. In Sec. III we describe the structural and physical assumptions in our model, in addition to the kinetic Monte Carlo algorithm used to simulate benzene mobility in Na-Y. In Sec. IV we present the calculated orientational cor-

a)Author to whom correspondence should be addressed.

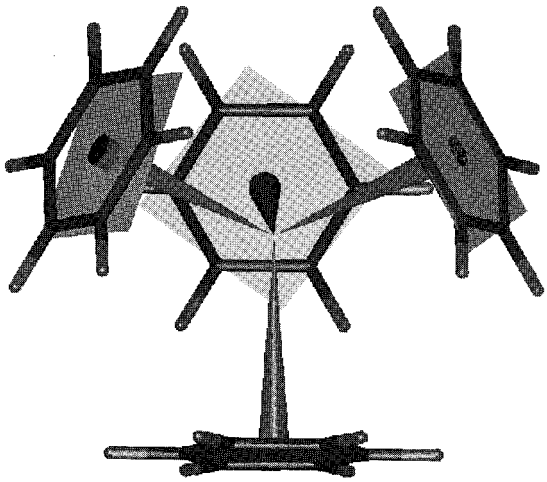

FIG. 1. Schematic of tetrahedrally arranged benzene binding sites in Na-Y.

relation functions and mean square displacements, and compare the information they provide regarding benzene mobility and zeolite structure. Finally, in Sec. V we give concluding remarks emphasizing the experimental implications of our theoretical findings.

II. NMR ORIENTATIONAL CORRELATION FUNCTIONS

The importance of orientational correlation functions (OCFs) for modeling and interpreting NMR measurements of molecular reorientation dynamics has been discussed by several authors.[9,15–17] Here we give a brief review to summarize how our computational results for benzene in Na-Y can be compared with experiment. We begin with the work of Boddenberg *et al.*[9,18] who derived an OCF accounting for rotational diffusion about benzene's six-fold axis (S), libration of the six-fold axis (L), and rotational diffusion of the six-fold axis on a sphere (D). The resulting OCF is[9]

$$C(t)=e^{-t/\tau_D}\sum_{m=-2}^{+2} f_m e^{-m^2 t/6\tau_S} \times[g^2+(1-g^2)e^{-(1-m^2/6)t/\tau_L}], \tag{2.1}$$

where f_m is a geometrical factor and g measures the mean square librational amplitude of the six-fold axis. While this formulation is useful for characterizing benzene mobility on, e.g., platinum microcrystallites,[9] it is too simple to treat benzene orientational randomization (BOR) in Na-Y zeolite. Indeed, on a typical time scale of BOR in a Na-Y, τ_S and τ_L are so short that Eq. (2.1) reduces to $C(t) = f_0 g^2 e^{-t/\tau_D}$. We show below that since benzene jumping in Na-Y is very different from rotational diffusion on a sphere, BOR in Na-Y can exhibit multi-exponential decay of the OCF, providing information regarding intracage motion, diffusion and cation distributions in zeolites.

Benzene jumps among tetrahedrally arranged sites in Na-Y,[4,19] shown schematically in Fig. 1, giving rise to ''pseudo-isotropic'' motion because tetrahedral symmetry is high enough to give full orientational randomization. This similarity to isotropic motion suggests a useful starting point for the derivation of our OCF, while still allowing for multi-exponential decay. The OCF for benzene[20] in the isotropic limit[11] is given by[16]

$$C_j(t)=\sum_{m=-2}^{+2} f_{jm}(\theta)\langle D^{2*}_{m,0}(\Phi_0,\Theta_0,0)D^2_{m,0}(\Phi_t,\Theta_t,0)\rangle, \tag{2.2}$$

where $\langle\cdots\rangle$ denotes an ensemble average, $D^j_{m,m'}(\alpha,\beta,\gamma)$ is a Wigner rotation matrix element[21] and (Φ_t,Θ_t) are spherical polar angles which transform between a molecular axis (i.e., the principal z-axis) at time t and the Zeeman field axis $\vec{\mathbf{B}}_0$. The coefficients $f_{jm}(\theta) = [D^2_{j,m}(0,\theta,0)]^2$ where θ is the angle between a zeolite crystallite principal z-axis and the $\vec{\mathbf{B}}_0$ field axis. Averaging the $f_{jm}(\theta)$ coefficients over a Na-Y powder composed of randomly oriented zeolite crystallites gives a j- and m-independent factor. Setting this factor to unity normalizes the OCF obtained below. Equation (2.2) can then be expressed entirely in the molecular frame by noting that the sum over m renders the OCF a function only of the molecular rotation angle between (Φ_0,Θ_0) and (Φ_t,Θ_t). We demonstrate this using the spherical harmonic addition theorem[21] where $D^j_{m,0}(\alpha,\beta,0) = \sqrt{4\pi/(2j+1)}Y^*_{j,m}(\beta,\alpha)$ and $Y_{j,m}(\beta,\alpha)$ is a spherical harmonic.[21] Equation (2.2) thus becomes

$$C(t)=\sqrt{\frac{4\pi}{5}}\left\{\sqrt{\frac{4\pi}{5}}\sum_{m=-2}^{2}\langle Y_{2,m}(\Theta_0,\Phi_0)Y^*_{2,m}(\Theta_t,\Phi_t)\rangle\right\} = \sqrt{\frac{4\pi}{5}}\langle Y_{2,0}(\beta_t,0)\rangle=\langle P_2(\cos\beta_t)\rangle, \tag{2.3}$$

where $P_2(x) = \frac{1}{2}(3x^2-1)$ is the second-degree Legendre polynomial, β_t is the angle between molecular axes at time 0 and t and the second equality in Eq. (2.3) is the spherical harmonic addition theorem.[21] The angle β_t is taken between benzene's six-fold axis at time 0 and t. The final form obtained in Eq. (2.3) is the working formula used in our kinetic Monte Carlo simulations described below. We note that Klein *et al.*[22] studied this OCF and others in their molecular dynamics simulations of benzene, xylenes and nitroaniline in Na-Y.

This OCF is related to several NMR probes of molecular reorientation in solids.[9,15–17] In deuterium spin-lattice relaxation, for example, which results from the interaction of a quadrupolar nucleus (^{2}H) and a stochastically fluctuating molecular electric field gradient, the spin-lattice relaxation rate T_1^{-1} is related to the OCF *via*

$$\frac{1}{T_1}=\frac{3}{16}C_Q^2[j(\omega_0)+4j(2\omega_0)], \tag{2.4}$$

where the spectral density, $j(\omega)$, is given by

$$j(\omega)=2\int_0^\infty dt\,\cos\,\omega t C(t). \tag{2.5}$$

In Eq. (2.4), C_Q is the quadrupolar coupling constant[9] and ω_0 is the Larmor frequency. As such, deuterium spin-lattice relaxation is sensitive to the Fourier transform of the OCF at multiples of the Larmor frequency. To extract an orientational randomization time scale one usually assumes that the OCF is an exponential and solves the following equation for the NMR correlation time τ_c:

$$\frac{1}{T_1}=\frac{3}{16}C_Q^2\left[\frac{\tau_c}{1+(\omega_0\tau_c)^2}+\frac{4\tau_c}{1+(2\omega_0\tau_c)^2}\right]. \tag{2.6}$$

While it is possible in principle to extract multi-exponential OCFs from NMR relaxation data,[9,23] a more direct measurement of the OCF would be preferable.

Two-dimensional exchange NMR spectroscopy, developed for studying polymer dynamics[17] and subsequently applied to benzene mobility in Ca-X,[24,25] directly measures the OCF and one molecular jumping angle. This method is suitable for studying reorientation dynamics in systems with $\tau_c \geqslant 1$ ms, such as benzene in Ca-X and Ca-Y.[17,24,25] The two-dimensional exchange spectrum, $S(\omega_1,\omega_2;t)$, consists of on-diagonal and off-diagonal components. The off-diagonal spectrum arises from molecules executing trajectories during the mixing time t involving initial and final states with different resonance frequencies.[26] The on-diagonal spectrum arises from molecules that either do not jump during the mixing time, or that execute trajectories in time t involving initial and final states with the same resonance frequency. In this context the OCF in Eq. (2.3) is given by[17]

$$C(t)=\frac{5}{\delta^2}\int d\omega_1\int d\omega_2\omega_1\omega_2 S(\omega_1,\omega_2;t), \tag{2.7}$$

where δ is a measure of the chemical shift. We emphasize that while NMR spin-lattice relaxation probes only select Fourier components of the OCF, two-dimensional exchange NMR directly measures the OCF for a wide variety of systems. This is particularly important for systems exhibiting complicated orientational randomization, such as benzene in the Na-Y zeolites modeled below.

An alternative but equivalent formula for the OCF is obtained by defining $p_{on}(t)$ and $p_{off}(t)$ as the normalized, integrated on-diagonal and off-diagonal spectral intensities, respectively, such that $p_{on}(t)+p_{off}(t)=1$ for all t. The OCF is then given by

$$C(t)=p_{on}(t)P_2(\cos\beta_{on})+p_{off}(t)P_2(\cos\beta_{off}). \tag{2.8}$$

For the tetrahedrally symmetric case of benzene in Na-Y, $P_2(\cos\beta_{on})=1$ and $P_2(\cos\beta_{off})=-\frac{1}{3}$. Using the normalization condition, the OCF becomes

$$C(t)=1-\tfrac{4}{3}p_{off}(t). \tag{2.9}$$

This formula provides a simple interpretation of the integrated spectral intensities. Indeed, at very short times $p_{off}(t)\cong p_{hop}(t)=1-e^{-k_{hop}t}\cong k_{hop}t$ where k_{hop} is the most facile process leading to benzene orientational randomization. This argument shows how the short time rise of off-diagonal intensity decreases the OCF from unity. Furthermore, the asymptotic limit of $p_{off}(t)$ is $\frac{3}{4}$ because of tetrahedral symmetry, showing that the eventual rise of off-diagonal intensity gives complete decay of the OCF. Finally, the phenomenon of anticorrelation, i.e., a particular disposition for hopping at certain intermediate times, corresponds to $p_{off}(t)$ exceeding $\frac{3}{4}$. Below we perform OCF calculations using Eqs. (2.3) and (2.9) to demonstrate their numerical equivalence for benzene in Na-Y.

III. THEORETICAL METHODOLOGY

In the present article we model benzene orientational randomization (BOR) at infinite dilution in Na-Y (Si:Al $\geqslant$2.0). Below we describe various structural and physical assumptions of our model, in addition to the kinetic simulation techniques used to perform the ensemble average in Eq. (2.3). We then summarize the theoretical methodology at the end of this section.

A. Benzene in Na-Y (Si:Al=2.0)

Benzene mobility in Na-Y strongly depends upon the number and placement of Na(II) cations in the zeolite framework structure.[4,11,19,27–30] It is therefore important when discussing benzene mobility in a particular Na-Y to quantify the Na(II) occupancy, in addition to standard properties such as the Si:Al ratio. For example, a Si:Al ratio of 2.0 requires 64 ions per unit cell to balance the negative framework charge. In this case we assume[4,5] full occupation of Na sites I′ (32 per unit cell, located in smaller β cages) and Na sites II (32 per unit cell, 4 per supercage on the vertices of a tetrahedron). This occupancy model is reasonable considering that only the Na(II) ions are accessible to a penetrant the size of benzene. In addition, diffraction studies of Na-Y (Si:Al=1.7)[31] and Na-Y (Si:Al=2.4)[19] find nearly full Na(II) occupation. Before discussing Na(II) occupancy models for other Si:Al ratios, we describe the binding sites, hopping paths and kinetic simulation techniques used to calculate the OCF for benzene in Na-Y (Si:Al=2.0).

Our previous MD-DOCKER calculations find two distinct binding sites for benzene in Na-Y (Si:Al=2.0),[4,5] in agreement with the powder neutron diffraction results of Fitch *et al.*[19] The calculated sorption sites are shown in Fig. 2. In the S_{II} binding site, benzene is facially coordinated to a supercage 6-ring, 2.70 Å above Na(II). In the W site, benzene is centered in the 12-ring window, 5.3 Å from the S_{II} site. Because of the strong Na–benzene interaction, the S_{II} site is much more stable than the W site, by *ca.* 25 kJ mol^{-1} according to some estimates.[4,27–30]

For benzene in Na–Y (Si:Al=2.0), the calculated $S_{II}\leftrightarrow S_{II}$ and $S_{II}\leftrightarrow W$ minimum energy paths (MEPs) are shown in Figs. 3 and 5 with the corresponding energetics shown in Figs. 4 and 6, respectively. These MEPs were obtained using our coordinate driving method[4] with our recently fitted potential energy surface for benzene in faujasites.[4] These hopping paths clearly demonstrate the reorientation processes probed by NMR relaxation and two-dimensional exchange NMR. The calculated $S_{II}\rightarrow S_{II}$ activation energy is 35 kJ mol^{-1}, in reasonable agreement with 24

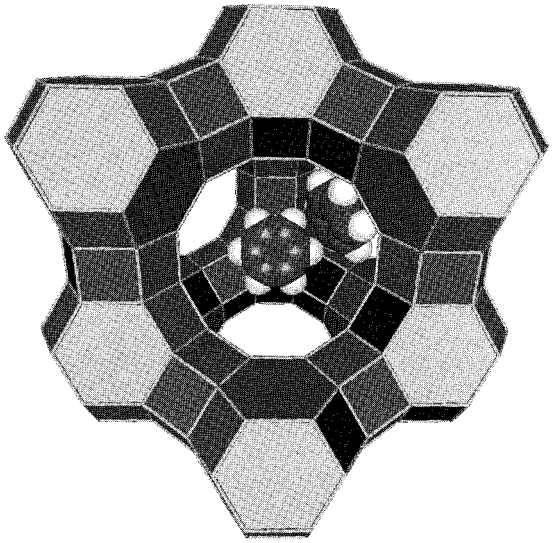

FIG. 2. Binding geometries of benzene in Na-Y. Central benzene is at S_{II} site, 2.7 Å above Na(II), with a binding energy of -75 kJ mol^{-1}. Upper right benzene is at the W site, 5.3 Å from the S_{II} benzene, with a binding energy of -50 kJ mol^{-1}.

kJ mol^{-1} obtained by NMR relaxation (*vide infra*).[11]

Our calculated hopping activation energies and hypothetical Arrhenius prefactors (*vide infra*), first reported in Ref. 4, are summarized in Table I. We note that leaving the W site is much more facile than leaving the S_{II} site in our model. Indeed, the predicted 300 K residence time at the S_{II} site is *ca*. 5000 times longer than that at the W site.

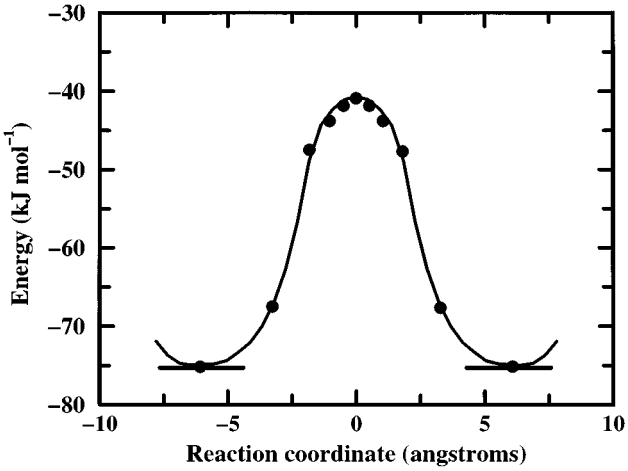

FIG. 4. $S_{II} \leftrightarrow S_{II}$ energetics with 35 kJ mol^{-1} activation energy.

B. Kinetic Monte Carlo

We apply the kinetic Monte Carlo (KMC) algorithm to benzene mobility in Na-Y by replacing the zeolite framework with a three-dimensional lattice of S_{II} and W binding sites. Such a lattice model is known to accurately reproduce mobilities when site residence times are much longer than travel times between sites.[13,32] This is indeed the case for benzene in cation-containing faujasites because of the strong charge–quadrupole interactions between Na(II) ions and benzene.[33] Connecting the S_{II} and W sites are four distinct hopping events, each with a characteristic rate coefficient: $k(S_{II} \rightarrow S_{II})$, $k(S_{II} \rightarrow W)$, $k(W \rightarrow S_{II})$ and $k(W \rightarrow W)$. The probability to make a particular hop is proportional to the associated rate coefficient.

We use a fixed time step KMC algorithm for OCF calculations in which a random hop is attempted at each time

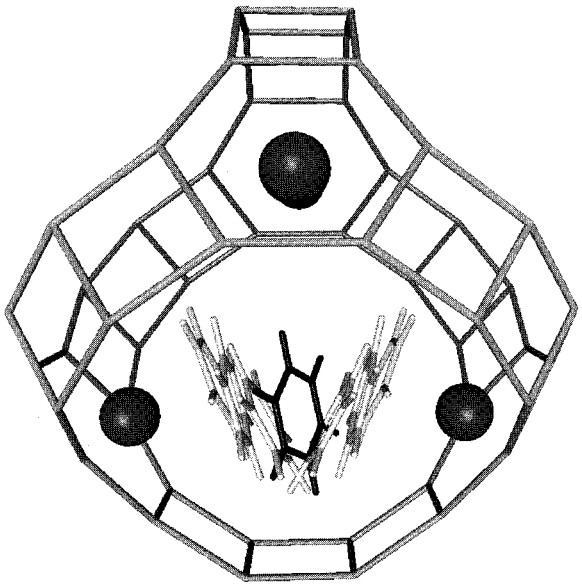

FIG. 3. $S_{II} \leftrightarrow S_{II}$ minimum energy path with a transition state indicated in bold face.

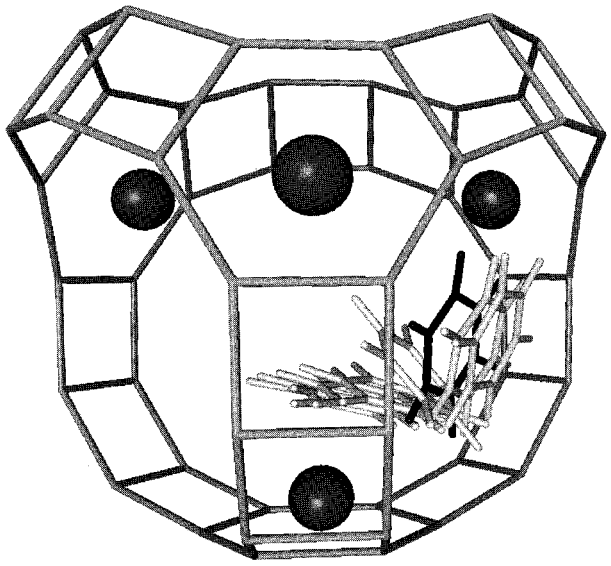

FIG. 5. $S_{II} \leftrightarrow W$ minimum energy path with a transition state indicated in bold face.

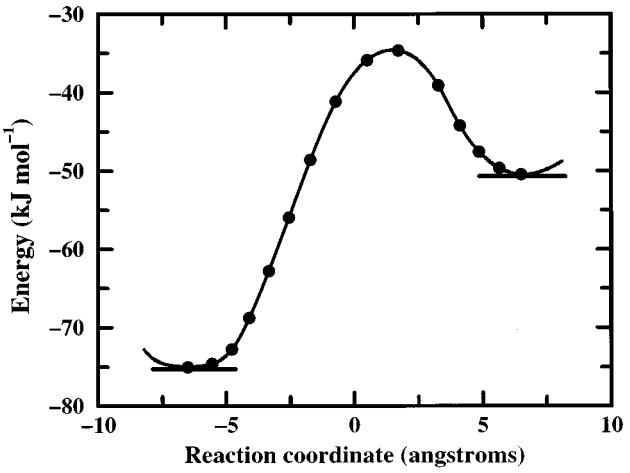

FIG. 6. $S_{II} \leftrightarrow W$ energetics with 41 kJ mol^{-1} activation energy.

step. The hop is accepted or rejected based on the kinetic Metropolis prescription in which a ratio of hopping rate coefficients, k_{hop}/k_{ref}, is compared to a random number. Here k_{ref} is a reference rate that controls the temporal resolution of the calculated OCF, i.e., $\delta t = 1/k_{ref}$ is the time bin width used for accumulating KMC statistics. During a KMC simulation benzene's orientation is stored at each time step $i = 1,\ldots,N$. The OCF is calculated as

$$C(t=n\,\delta t)=\frac{1}{N-n}\sum_{i=1}^{N-n} P_2[\vec{\mathbf{v}}(i)\cdot\vec{\mathbf{v}}(i+n)], \tag{3.1}$$

where $\vec{\mathbf{v}}(i)$ is the unit vector specifying the orientation at KMC step i. We note that calculating well converged OCFs for long times is computationally challenging because of the difficulty in obtaining proper cancellation of positive and negative $P_2(x)$ values from a Monte Carlo random walk.

We use a variable time step KMC algorithm for mean square displacement calculations in which a hop is made every KMC step and the system clock is updated accordingly.[34] The mean time elapsed before each hop is the inverse of the *total* rate coefficient to leave the originating site.[34] For example, if benzene in Na-Y (Si:Al=2.0) jumps from an S_{II} site, the mean time elapsed is

$$\Delta t(S_{II})=\frac{1}{3[k(S_{II}\rightarrow S_{II})+k(S_{II}\rightarrow W)]}, \tag{3.2}$$

where the factor of three counts available target sites in the Na-Y supercage structure. Since rate coefficients for leaving the S_{II} site are typically much smaller than those for leaving the W site, the elapsed S_{II} time is much larger than the elapsed W time. Thus, the variable time step KMC random walk algorithm efficiently models both sluggish and rapid motions in the Na-Y–benzene system. Ensemble averages required for calculating mean square displacements are performed as previously described in Ref. 4. In order to resolve translational dynamics over widely separated length and time scales we display mean square displacements with log–log plots. In these cases it is computationally advantageous to perform the ensemble average using logarithmic time bins as previously discussed in Ref. 6.

TABLE I. Hopping activation energies and hypothetical Arrhenius prefactors for benzene in Na-Y. Our model predicts that leaving the W site is relatively facile.

Jump	Activation energy (kJ mol^{-1})	Arrhenius prefactor (s^{-1})
$S_{II}\rightarrow S_{II}$	35	10^{13}
$S_{II}\rightarrow W$	41	10^{13}
$W\rightarrow S_{II}$	16	10^{13}
$W\rightarrow W$	18	10^{13}

In Refs. 4, 5, and 6 and in the present study, we estimate rate coefficients using the Arrhenius formula in which $k \cong \nu e^{-\beta E_a}$, where ν and E_a are temperature independent. We assume that the Arrhenius prefactors $\{\nu\}$ resemble typical vibrational frequencies, of order 10^{13} s^{-1}. We believe these rate coefficients are sufficiently accurate for the purpose of drawing qualitative conclusions. We calculate activation energies for a particular hop by following the MEP from an initial site, through the transition state, to the final site (cf. Figs. 3, 4, 5, and 6). For a full description of the MEP calculation, please see Ref. 4.

C. Benzene in Na–Y (Si:Al>2.0)

Benzene mobility in Na-Y (Si:Al>2.0) differs from that in Na-Y (Si:Al=2.0) because changing the Si:Al ratio alters Na(II) occupancy.[4,11,19,27–30] Since occupancies of different Na^+ sites vary differently upon changing the Si:Al ratio, depending on site stabilities and zeolite synthesis conditions, no simple formula is known that relates Na(II) occupancy to the Si:Al ratio. Below we model the behavior of benzene orientational randomization in Na-Y as Na(II) occupancy is decreased. In order to express these results in terms of the Si:Al ratio, a standard zeolite composition variable, we assume full Na(I′) occupation for Si:Al>2.0 as we did for Si:Al=2.0.[4,5] We emphasize that this assumption is *not* crucial for the conclusions we draw below; rather it allows us to label a particular Na(II) occupancy in Na-Y by its Si:Al ratio. In an experimental verification of our computational results, structural information about the zeolite would have to be measured, in addition to the OCF, quantifying the site II cation occupancy.

Figure 7 shows how Na(II) occupancy varies with the Si:Al ratio in our model. We have calculated benzene diffusion coefficients for systems marked by circles (empty and filled) in Fig. 7, and have compared benzene mean square displacements to OCFs for systems marked by filled circles in Fig. 7. We note that by assuming full Na(I′) occupancy for all Si:Al ratios, benzene mobility in our model increases precipitously near Si:Al=5.0 as the last Na(II) cation is removed. Such a sudden mobility increase is an artifact of our cation occupancy model, and is not to be taken seriously.

We model BOR in Na-Y for a given Si:Al ratio, and hence for a given Na(II) occupancy, by replacing the zeolite framework with a three-dimensional lattice of S_{II} and W benzene binding sites, where the number of S_{II} sites is ob-

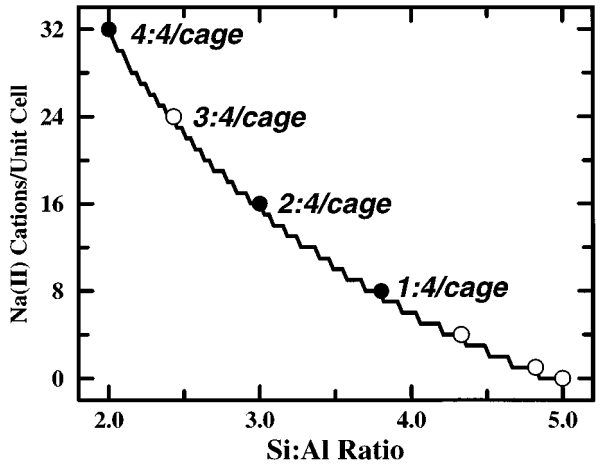

FIG. 7. Model Na(II) occupancy vs Na-Y Si:Al ratio. Benzene diffusion coefficients are reported below for all circles (empty and filled), and are compared with results from OCFs for filled circles.

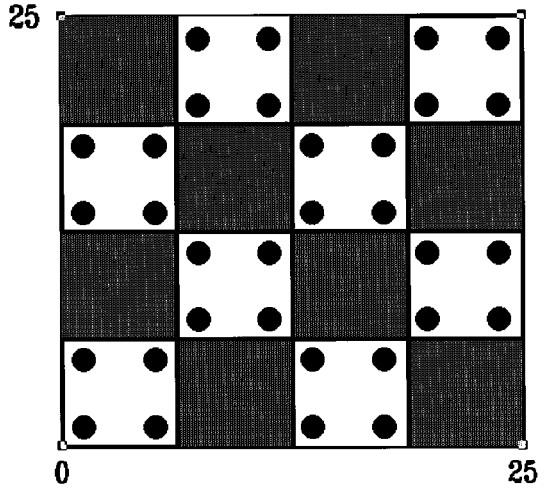

FIG. 8. Schematic of Na-Y (Si:Al=2.0) unit cell ($a \approx 25$ Å) where shaded boxes are β cages, unshaded boxes are supercages and black dots are Na(II) cations.

tained from Fig. 7. This model ignores benzene binding at supercage 6-rings with no associated Na(II) cation. This is a very good approximation because benzene residence times at these 6-rings are significantly shorter than the times required for full BOR. As such, benzene visiting 6-rings without Na(II) cations would contribute negligibly to the ensemble average in Eq. (2.3). From an experimental perspective, benzene rotational dynamics at these ''siliceous'' 6-rings is too fast to be observed by two-dimensional exchange NMR,[24,25] and is on the borderline for NMR relaxation.[11]

Two aspects of our model for BOR in Na-Y (Si:Al >2.0) need to be discussed: determining spatial patterns of Na(II) occupancy and calculating rate coefficients for hopping between these sites. Regarding the latter, we assume that the activation energy for hopping between S_{II} sites in a supercage where some Na(II) cations are missing is *unaffected* by cation vacancies, i.e., takes the value for benzene in Na–Y (Si:Al=2.0). In addition, we assume that activation energies for $S_{II} \leftrightarrow W$ and $W \leftrightarrow W$ jumps are likewise unaffected by cation vacancies. This approximation, which derives from analyzing Na(II)–benzene charge–quadrupole interactions varying as $1/r^3$,[35] is expected to affect activation energies by roughly 15–20% because of the length scales involved.[36] For benzene in Na-Y (Si:Al=2.0), the calculated $S_{II} \leftrightarrow S_{II}$ transition state benzene center of mass is ca. 5 Å from an initial or final Na(II) cation, and is ca. 9 Å from either of the other two Na(II) cations. Removing one or both of these distant cations is not expected to drastically change activation energies; similar arguments apply for the other jumps. We note that this approximation, which gives error on par with our initial minimum energy path calculations,[4] drastically simplifies the interpretation of KMC simulations by reducing the number of fundamental rate processes involved. In future studies we plan to examine the effect on jumping rates from heterogeneous supercage environments.

Determining accurate spatial patterns of Na(II) occupancy for Na-Y (Si:Al>2.0) is challenging because of the difficulty in measuring and calculating Al and Na^+ distributions in disordered zeolites. Since cation mobilities in dehydrated zeolites are significantly smaller than benzene mobilities,[37–39] Na(II) disorder is static on the time scale of BOR. We turn this difficulty to our advantage by proposing that benzene mobility can be used to probe static Na(II) disorder. That is, while we do not know the proper spatial Na(II) occupancy pattern, we can calculate benzene mobilities assuming various occupancy patterns to determine measurable signatures for these patterns.

We examine two such patterns below, both based on random Na(II) siting. The first pattern, called ''cage'' disorder, assumes that each supercage has roughly the same number of Na(II) cations. For example, a Si:Al ratio of 3.0 gives on average two Na(II) cations per supercage. The cage disorder pattern requires that each supercage has exactly two Na(II) cations, placed randomly at two of the four possible tetrahedrally arranged sites. This pattern would arise physically from, e.g., a random distribution of framework Al with density fluctuations on a length scale smaller than the supercage dimension, and Na ions in close proximity to framework Al. Although this spatial distribution seems plausible, it imposes constraints which may be artificial. A less constrained pattern, called ''cell'' disorder, randomly places Na(II) cations in the Na-Y cubic unit cell.

Schematic illustrations of cage and cell disorder are shown in Figs. 8, 9 and 10. Figure 8 depicts the Na-Y (Si:Al $=2.0$) unit cell containing 8 supercages and 8 β cages. The shaded boxes are β cages containing no Na(II) cations, and the unshaded boxes are supercages containing four Na(II) cations (black dots) because Si:Al=2.0. Figure 9 shows cage disorder for Na-Y (Si:Al=3.0), with 16 Na(II) cations per unit cell randomly distributed so that each supercage contains two ions. Figure 10 shows cell disorder for Na-Y (Si:Al $=3.0$), involving 16 Na(II) cations randomly distributed over the unit cell, in this case giving one supercage with no Na(II) cations and one supercage with four cations. We emphasize that our KMC simulations of benzene in Na-Y (Si:Al$\geqslant 2.0$)

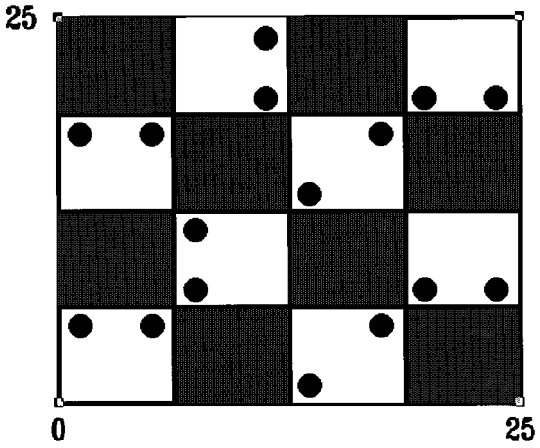

FIG. 9. Schematic of Na-Y (Si:Al=3.0) unit cell showing cage disorder: all supercages have two Na(II) cations randomly placed within each supercage.

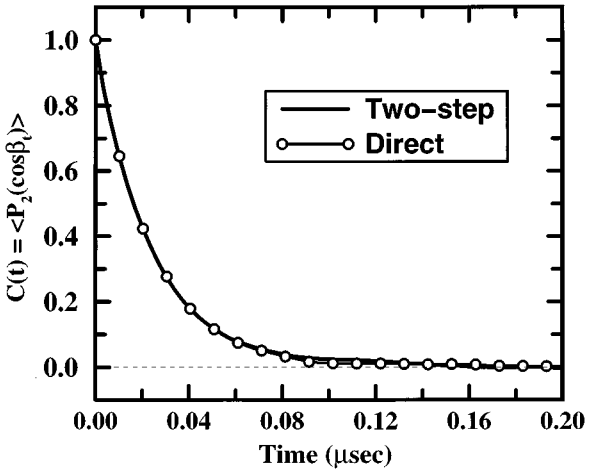

FIG. 11. KMC calculated OCF for benzene in Na-Y (Si:Al=2.0) at $T=300$ K comparing ''direct'' and ''two-step'' methods.

use the actual Na-Y structure for constructing lattices of S_{II} and W benzene binding sites.

D. Summary of theoretical methodology

We model benzene orientational randomization (BOR) in Na-Y for a given Si:Al ratio, and hence for a given Na(II) occupancy, by replacing the zeolite framework with a three-dimensional lattice of S_{II} and W benzene binding sites where the number of S_{II} sites is obtained from Fig. 7. S_{II} sites are placed randomly according to either cage or cell disorder. We use fixed time step kinetic Monte Carlo (KMC) for calculating OCFs according to Eqs. (2.3) and (3.1), and also variable time step KMC for calculating mean square displacements according to Eq. (3.2) and Ref. 4. Activation energies used to compute hopping rate coefficients for benzene in Na-Y (Si:Al$>$2.0) are estimated from minimum energy path calculations performed for benzene in Na-Y (Si:Al $=$2.0). The results are examined to determine which underlying jumps control BOR, the extent to which OCFs and mean square displacements contain complementary information, and the effect of static Na(II) disorder on benzene mobilities.

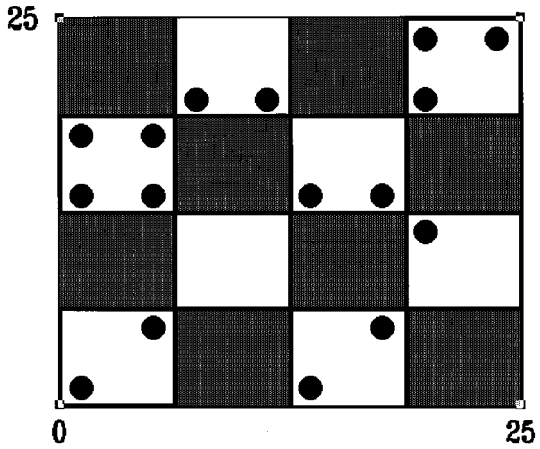

FIG. 10. Schematic of Na-Y (Si:Al=3.0) unit cell showing cell disorder: 16 Na(II) cations randomly distributed over the unit cell.

IV. RESULTS AND DISCUSSION

We now discuss the results of our KMC simulations of benzene mobility in Na-Y (Si:Al$\geqslant$2.0). After discussing the calculated OCFs and mean square displacements, we compare the information they provide regarding benzene mobility and zeolite structure.

A. Orientational correlation functions

Benzene in Na-Y (Si:Al=2.0). Since BOR in Na-Y arises from a variety of fundamental hopping processes, KMC simulations are useful for determining which hopping process, if any, controls BOR rates. Figure 11 shows the KMC calculated OCF for benzene in Na-Y (Si:Al=2.0) at $T=300$ K comparing two computational approaches. The ''direct'' calculation involves using KMC to evaluate the ensemble average in Eq. (2.3). The ''two-step'' approach involves first using KMC to calculate $p_{off}(t)$, the probability at time t that benzene gives off-diagonal intensity, neglecting spin diffusion,[26] in two-dimensional exchange NMR; followed by substituting $p_{off}(t)$ into Eq. (2.9). The two methods give essentially exact agreement, confirming the interpretation in Eq. (2.8) of on- and off-diagonal spectral intensities. The OCF in Fig. 11 exhibits exponential decay, which arises from pseudo-isotropic motion giving full orientational randomization.

In order to extract quantitative BOR rates, we show $\ln|C(t)|$ in Fig. 12. The difficulty in using Monte Carlo to give proper sign cancellation for long times is evident in Fig. 12. Analyzing the short time slopes in Fig. 12 indicates that $k_{\mathrm{BOR}}= 1.3/\Delta t(\mathrm{S}_{II})$, where k_{BOR} is the BOR rate and $\Delta t(\mathrm{S}_{II})$ is the mean residence time at the S_{II} site given in Eq. (3.2). The factor of 1.3 can be understood as follows. For short times the OCF satisfies $C(t) \cong 1-\frac{4}{3}k_{hop}t$ as discussed in Eq. (2.9), where $k_{hop} = k(\mathrm{S}_{II}) = 1/\Delta t(\mathrm{S}_{II})$. The OCF in

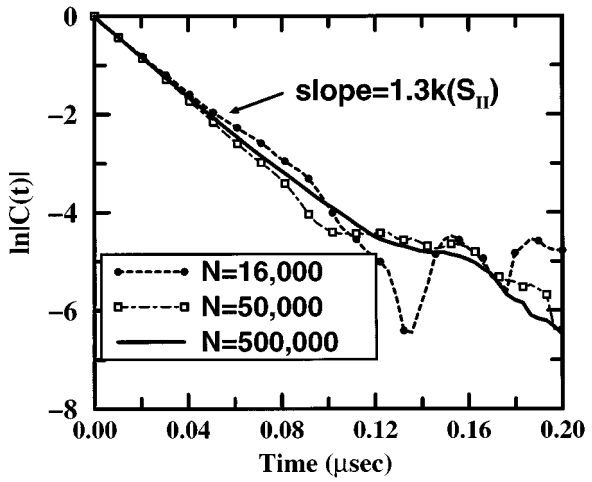

FIG. 12. Logarithm of Fig. 11 showing simple exponential decay for $C(t) \geqslant 0.01$ and statistical error thereafter.

Fig. 12 calculated from 500,000 KMC steps is a single exponential down to $C(t)=0.01$, suggesting that for longer times the short time approximation can be re-exponentiated to yield $C(t) = e^{-(4/3)k_{hop}t}$. As such, one would expect $k_{\mathrm{BOR}} = \frac{4}{3}k(\mathrm{S}_{II}) \cong 1.3k(\mathrm{S}_{II})$, in agreement with our numerical results. This argument does not suggest that we expect single exponential decay in all cases, but does explain the decay rate magnitude when single exponential decay is found.

The BOR rate found in Fig. 12 satisfies $k_{\mathrm{BOR}} = 1.3k(\mathrm{S}_{II}) \cong 4[k(\mathrm{S}_{II}\rightarrow\mathrm{S}_{II}) + k(\mathrm{S}_{II}\rightarrow\mathrm{W})] \cong 4k(\mathrm{S}_{II}\rightarrow\mathrm{S}_{II})$, where the final expression results from $k(\mathrm{S}_{II}\rightarrow\mathrm{S}_{II}) \gg k(\mathrm{S}_{II}\rightarrow\mathrm{W})$ at $T=300$ K in our model. This BOR rate expression can be identified as the number of mutually accessible sites multiplied by the site-to-site hopping rate coefficient, as previously discussed by Torchia and Szabo.[16] This analysis clearly indicates that BOR is dominated by intracage motion when this motion is significantly faster than cage-to-cage migration. Thus, we predict that the NMR spin-lattice relaxation experiments of Bull *et al.*[11] on benzene in Na-Y (Si:Al=1.7) observe intracage hopping processes, their data providing a direct probe of the $\mathrm{S}_{II}\rightarrow\mathrm{S}_{II}$ hopping rate coefficient. This suggests the comparison of their 24 kJ mol^{-1} apparent activation energy to our $E_a(\mathrm{S}_{II}\rightarrow\mathrm{S}_{II}) = 35$ kJ mol^{-1} as mentioned above.

In several instances self diffusion coefficients for adsorbed benzene are estimated from relaxation data[8–11] according to $D_{self} \sim D_{\mathrm{BOR}} = \frac{1}{6}k_{\mathrm{BOR}}a^2$, where a is a likely jump length chosen from structural data. Our present results suggest that using NMR relaxation data to estimate diffusivities may be incorrect for certain systems. Indeed, we find that BOR in Na-Y (Si:Al=2.0) is controlled by the intracage, $\mathrm{S}_{II}\rightarrow\mathrm{S}_{II}$ jump. We have previously found that benzene diffusion in this system is controlled by the cage-to-cage, $\mathrm{S}_{II}\rightarrow\mathrm{W}$ jump.[4,6] Therefore, reporting NMR correlation times in terms of diffusion coefficients may lead to inappropriate comparisons with data from, e.g., pulsed field gradient (PFG) NMR which directly measures mean square displacements.[1,7] Experimental verification of these predictions for benzene in Na-Y is not yet available because of the difficulty in measuring reliable self diffusion coefficients for benzene in Na-Y powders, which are composed of relatively small crystallites.[40]

Diffusion coefficients obtained from NMR relaxation data[8,10] agree remarkably well with those from PFG NMR[7,41] for benzene in Na-X, a zeolite similar to Na-Y but with more Na^+ ions per supercage. This close agreement is puzzling considering the analysis above for benzene in Na-Y. We have recently performed calculations indicating that these additional Na^+ ions affect both intracage and intercage hopping activation energies, making them approximately equal.[5] As such, although comparing D_{self} to D_{BOR} is generally inappropriate, it happens to give good agreement for *this* system because of fortuitous equivalence between intracage and intercage hopping time scales.

We close our discussion of BOR in Na-Y (Si:Al=2.0) by relating our calculated OCF to recent two-dimensional exchange spectra for benzene in Ca-X (Si:Al=1.0) measured by Chmelka and co-workers.[24,25] Powder neutron diffraction and X-ray diffraction studies[42] of this zeolite find nearly full occupation of Ca(II) sites (32 per unit cell, 4 per supercage on the vertices of a tetrahedron), in analogy with Na(II) cations in Na-Y. As such, benzene in Ca-X (Si:Al=1.0) jumps among tetrahedrally arranged sites *via* $\mathrm{S}_{II}\rightarrow\mathrm{S}_{II}$ and $\mathrm{S}_{II}\rightarrow\mathrm{W}$ hops, in analogy with motion in Na-Y. The relevant difference between benzene in Na-Y and in Ca-X is that adsorption heats and hopping activation energies are greater in Ca-X because of the approximately doubled charge on Ca ions. In order to model this system more closely, we have calculated MEPs for benzene in Ca-X (Si:Al=1.0).[43] Hopping activation energies extracted from these MEPs suggest that $k(\mathrm{S}_{II}\rightarrow\mathrm{S}_{II}) \gg k(\mathrm{S}_{II}\rightarrow\mathrm{W})$ at $T=300$ K, as was predicted for benzene in Na-Y. These results indicate that BOR is qualitatively identical in the two zeolites, i.e., $C(t)$ $\mathrm{C(t)}=e^{-(4/3)k_{hop}t}$ where $k_{\mathrm{BOR}}=\frac{4}{3}k_{hop}\cong 4k(\mathrm{S}_{II}\rightarrow\mathrm{S}_{II})$ for benzene in Ca-X.

The elegant measurements by Chmelka and co-workers[24,25] have revealed that benzene jumps among four tetrahedrally arranged sites and that the OCF decays exponentially. Their measured decay rates exhibit Arrhenius temperature dependence with the parameters $\nu(\mathrm{S}_{II}\rightarrow\mathrm{S}_{II}) = 10^{11}$ s^{-1} and $E_a(\mathrm{S}_{II}\rightarrow\mathrm{S}_{II}) = 62$ kJ mol^{-1}. These experiments represent some of the most detailed microscopic studies to date of molecular mobility in zeolites. Our calculations have helped to interpret the NMR spectra by resolving ambiguities regarding the jump assignment. Since the exchange spectrum relates to $\langle P_2(\cos\beta_t)\rangle$, an even function of $\cos\beta_t$, the experiment is unable to distinguish between jump angles β_t and $180° - \beta_t$. The symmetry of Na-Y and Ca-X is such that the intracage $\mathrm{S}_{II}\rightarrow\mathrm{S}_{II}$ jump angle is ca. 109.5°, while the intercage $(\mathrm{S}_{II})_{cage1}\rightarrow(\mathrm{S}_{II})_{cage2}$ jump angle is ca. 70.5°, precluding assignment of the BOR rate in terms of a fundamental hopping process. Our prediction[43] that $k(\mathrm{S}_{II}\rightarrow\mathrm{S}_{II}) \gg k(\mathrm{S}_{II}\rightarrow\mathrm{W})$ suggests that two-dimensional exchange spectra for benzene in Ca-X are controlled by *intracage* BOR.

Benzene in Na-Y (Si:Al=3.0). The preceding discussion pointed to the difficulty in experimentally disentangling

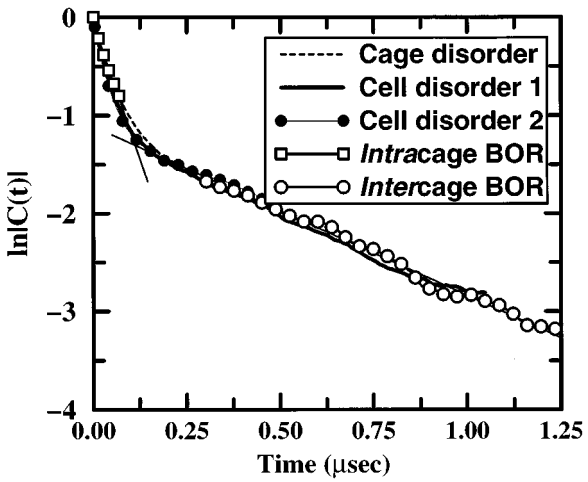

FIG. 13. $\ln|C(t)|$ for benzene in Na-Y (Si:Al=3.0) at $T=300$ K, showing insensitivity to the Na(II) occupancy pattern. Intracage motion gives rapid, incomplete decay while cage-to-cage migration gives slower, long time decay.

benzene intracage motion from intercage motion in zeolites. In this section we demonstrate that studying BOR in Na-Y with half Na(II) occupancy can unambiguously disentangle rates of intracage and intercage motion. Half Na(II) occupancy corresponds in Fig. 7 to Si:Al=3.0, although this point is not crucial as previously discussed. It is crucial, however, to determine the effect of different Na(II) occupancy patterns on benzene mobility. Figure 13 shows $\ln|C(t)|$ for benzene in Na-Y (Si:Al=3.0) at $T=300$ K, comparing several Na(II) occupancy patterns. The cage disorder system has two Na(II) ions per supercage, while the cell disorder systems have the patterns $(1, 0, 5, 2, 0)_{cell1}$ and $(0, 3, 3, 1, 1)_{cell2}$, where (n_0,n_1,n_2,n_3,n_4) signifies n_0 supercages with zero Na(II) ions, n_1 supercages with one Na(II) ion, etc. The results in Fig. 13 demonstrate remarkable insensitivity to particular occupancy patterns, suggesting that such an OCF should be measurable with, e.g., two-dimensional exchange NMR on benzene in Ca-Y with half Ca(II) occupancy. Below we interpret the nature of BOR in Na-Y (Si:Al=3.0) and suggest an explanation for the predicted insensitivity to the Na(II) disorder.

The OCF in Fig. 13 exhibits biexponential decay resulting from incomplete Na(II) occupancy. Considering first cage disorder, each supercage contains two S_{II} binding sites. Benzene hopping between these two sites gives *incomplete* decay of the OCF up to *ca.* 0.12 μs because the tetrahedral symmetry that was present with full Na(II) occupancy is broken with half Na(II) occupancy. The BOR rate extracted from short time decay is $k_{\mathrm{BOR}}=1.3k(\mathrm{S}_{II})=1.3[k(\mathrm{S}_{II}\rightarrow\mathrm{S}_{II})+3k(\mathrm{S}_{II}\rightarrow\mathrm{W})]\cong 1.3k(\mathrm{S}_{II}\rightarrow\mathrm{S}_{II})$. This BOR rate is one third of that found in Na-Y (Si:Al=2.0) because with two Na(II) ions per cage, there is only one target S_{II} site available as opposed to the three target S_{II} sites available with full Na(II) occupancy. In the absence of intercage motion the asymptotic value of $p_{off}(t)$ at long times would be $\frac{1}{2}$ because of the two S_{II} sites per supercage. As such, the OCF would plateau at $C(t)=1-\frac{4}{3}\cdot\frac{1}{2}=\frac{1}{3}$ or $\ln|C(t)| = -1.1$ as determined from Eq. (2.9). Figure 13 shows the transition from rapid to sluggish motion very near this value of the OCF.

In order to execute full orientational randomization with half Na(II) occupancy, benzene must visit enough supercages to sample all four tetrahedral orientations. The long time BOR rate is thus controlled by the rate of cage-to-cage motion. Indeed, the BOR rate extracted from long time decay in Fig. 13 is $k_{\mathrm{BOR}}=k_{cage}=\frac{1}{2}\cdot 4\cdot k(\mathrm{S}_{II}\rightarrow\mathrm{W})$ where k_{cage} is the intercage hopping rate coefficient, i.e., $\tau_{cage}=1/k_{cage}$ is the mean supercage residence time. The factors of $\frac{1}{2}$ and 4 were previously explained in our recent theoretical studies of benzene diffusion in Na-Y.[4,6] The factor of $\frac{1}{2}$ accounts for randomizing in the W site which halves the probability to leave the cage. The factor of 4 accounts for the four ways to leave the supercage through one of the four windows. Since we have previously shown that $D_{self}=\frac{1}{6}k_{cage}a^2$ where $a\cong 11$ Å is the cage-to-cage length,[4,6] the OCF in Fig. 13 suggests a new approach for measuring self diffusion coefficients in zeolites.

Although much of the preceding discussion assumed cage disorder, especially our analysis of short time intracage BOR, the results in Fig. 13 are insensitive to particular occupancy patterns. We now examine this effect. Deviations from cage disorder encountered with cell disorder are expected to affect BOR rates in two ways. First, instead of having the intracage BOR rate $k_{\mathrm{BOR}}=1.3k(\mathrm{S}_{II}\rightarrow\mathrm{S}_{II})$, one expects a collection of intracage rates $k_{\mathrm{BOR}}(n)=1.3(n-1)k(\mathrm{S}_{II}\rightarrow\mathrm{S}_{II})$ where $n=1,\ldots,4$ is the Na(II) occupancy of a particular supercage. Since these jumps are independent processes, averaging different supercage occupancies during a KMC simulation is tantamount to averaging the corresponding rates, yielding $k_{\mathrm{BOR}}=\langle k_{\mathrm{BOR}}(n)\rangle=1.3(\langle n\rangle-1)k(\mathrm{S}_{II}\rightarrow\mathrm{S}_{II})=1.3k(\mathrm{S}_{II}\rightarrow\mathrm{S}_{II})$ because the average Na(II) occupancy is two per supercage. This explains the agreement between cage and cell disorder at short times.

The second effect from cell disorder pertains to the extent of intracage BOR once benzene begins cage-to-cage migration. For cages containing two Na(II) ions, one expects $C(t)\sim\frac{1}{3}$ at the onset of intercage motion as discussed above. Alternatively, supercages containing four Na(II) ions are likely to give full BOR before benzene exits the cage, while cages with only one Na(II) give no BOR before cage-to-cage motion.[44] Although the KMC algorithm averages these different environments during the simulation, the resulting OCF may not necessarily agree with that from cage disorder. Figure 13 indicates that cage and cell disorder give virtually identical OCFs, a somewhat surprising result. We speculate that with half Na(II) occupancy there are too many cations present for cell and cage disorder to give markedly different results. Indeed, we find in the next section that the situation changes significantly when considering one quarter Na(II) occupancy.

We close our discussion of BOR in Na-Y (Si:Al=3.0) by emphasizing the experimental implications of our theoretical predictions. We have suggested that by measuring the OCF for benzene in Na-Y with half Na(II) occupancy, one can simultaneously obtain the intracage hopping rate and the

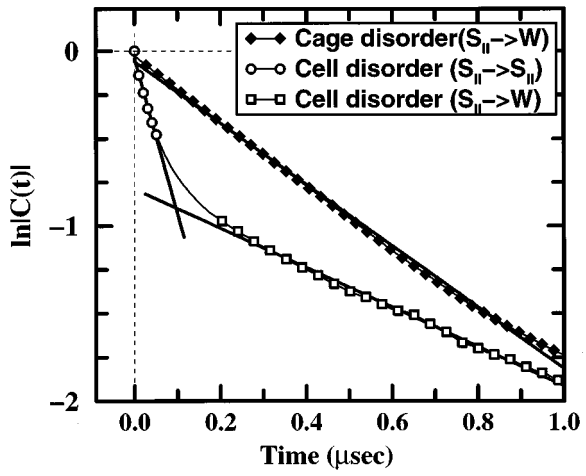

FIG. 14. $\ln|C(t)|$ for benzene in Na-Y (Si:Al=3.8) at $T=300$ K, showing qualitative sensitivity to the Na(II) occupancy pattern.

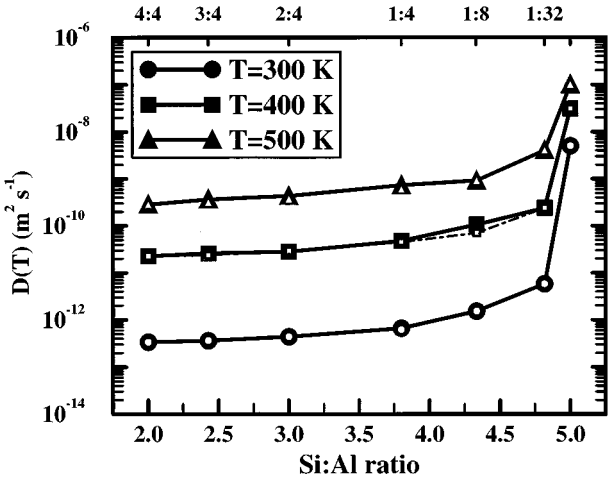

FIG. 15. Benzene diffusion coefficients for different temperatures and Si:Al ratios, showing insensitivity to cage disorder (large filled symbols) vs cell disorder (small empty symbols).

self diffusion coefficient. This is important for connecting the very different length scales probed by NMR relaxation and PFG NMR experiments. A convenient way to measure the predicted OCF for, e.g., benzene in Ca-Y with two-dimensional exchange NMR is first to focus on the rapid, short time decay. Once the intracage BOR rate is determined, one then focuses on diffusive time scales, thereby generating a relatively narrow peak along the diagonal arising from rapid intracage motion. This approach is complementary to PFG NMR because OCF measurements do not require large particles for reliable diffusion coefficients. We anticipate that such experiments will greatly enhance our understanding of molecular mobility in zeolites.

Benzene in Na-Y (Si:Al=3.8). In the preceding section we found that cage and cell disorder give very similar OCFs for benzene in Na-Y (Si:Al=3.0). While this insensitivity to particular Na^+ distributions lends credibility to the predicted OCF, it makes detecting different occupancy patterns very difficult. This is important because measuring the distribution of Na^+ ions is closely related to measuring Al distributions in disordered zeolites, which remains challenging to modern characterization methods.[45] In this section we demonstrate that studying BOR in Na-Y with one quarter Na(II) occupancy can clearly distinguish between cage and cell disorder.

One quarter Na(II) occupancy corresponds on average to one Na(II) per supercage, and in Fig. 7 to Si:Al=3.8. Figure 14 shows $\ln|C(t)|$ for benzene in Na-Y (Si:Al=3.8) at $T=300$ K, showing qualitative sensitivity to Na(II) occupancy patterns. Since cage disorder entails precisely one Na(II) in each cage, benzene must visit adjacent supercages to commence orientational randomization.[44] As such, the OCF exhibits single exponential decay controlled by the $S_{II}\rightarrow W$ rate coefficient. Indeed, for cage disorder $k_{BOR} = 2k(S_{II}\rightarrow W)$ as was found for long time BOR in Na-Y (Si:Al=3.0).

The cell disorder system in Fig. 14 has a (3, 2, 3, 0, 0) occupancy pattern, enabling partial intracage BOR because three supercages contain two Na(II) cations. Since full BOR in the cell disorder system requires cage-to-cage motion, biexponential decay arises as was predicted for benzene in Na-Y (Si:Al=3.0). Figure 14 also predicts a slight difference in the diffusion coefficients obtained from cage and cell disorder. The striking conclusion drawn from Fig. 14 is that studying BOR in Na-Y with one quarter Na(II) occupancy can clearly distinguish between qualitatively different Na^+ distributions.

We therefore suggest that guest mobility can be used to probe structural aspects of disordered zeolites. Two-dimensional exchange NMR can be used, e.g., to determine the supercage Ca^{+2} distribution pattern in Ca-Y with one quarter Ca(II) occupancy. By determining whether single exponential or biexponential decay is observed, the NMR spectra will point to either cage or cell disorder, respectively.

B. Mean square displacements

In Sec. IV A we predicted that studying orientational randomization in zeolites can provide valuable information about intracage motion, diffusion and cation disorder. One wonders whether such information can also be extracted from direct diffusion measurements such as PFG NMR or tracer exchange,[1] considering the wide application of these methods to mass transport in zeolites. We have previously argued that intracage hopping rates in Na-Y cannot be determined by measuring diffusivities because intracage motion does not contribute to long range diffusion.[4,5] It is possible, though, that diffusion measurements can be used to infer cation distributions. To address this issue, we have performed additional KMC simulations to calculate mean square displacements and self diffusion coefficients for all the systems discussed in Sec. IV A.

Figure 15 shows KMC calculated self diffusion coefficients for benzene in Na-Y for various temperatures and Si:Al ratios, comparing cage and cell disorder patterns designated by large filled symbols and small empty symbols, respectively. The results in Fig. 15 predict that benzene dif-

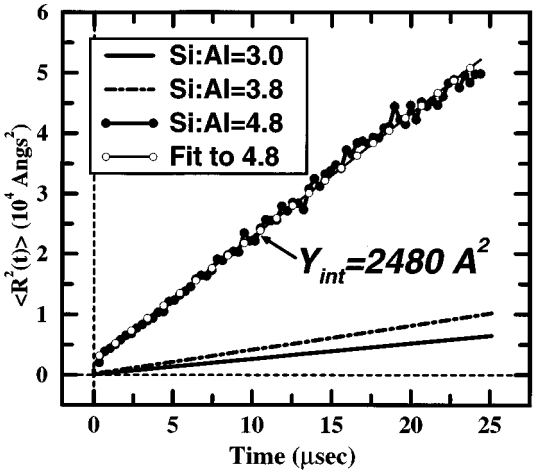

FIG. 16. Benzene mean square displacements in Na-Y at $T=300$ K for Si:Al=3.0, 3.8 and 4.8. The sizable y-intercept for Si:Al=4.8 is explained below.

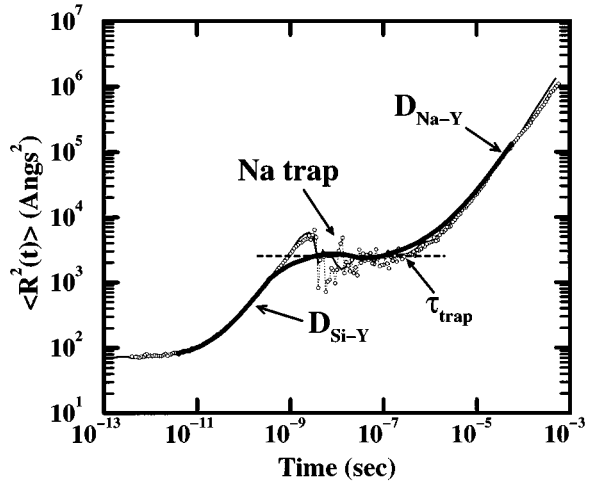

FIG. 17. Log–log plot of Fig. 16 for Si:Al=4.8 showing rapid diffusion at short times, followed by dormancy at the lone S_{II} site, and finally normal diffusion giving the mean square displacement in Fig. 16 and the diffusion coefficient in Fig. 15.

fusion coefficients increase monotonically with the Na-Y Si:Al ratio, and that the increase is gentle for Si:Al=2.0–4.0 and more steep near Si:Al=5.0 (cf. Sec. III C). The diffusion coefficients for Si:Al=2.0–4.0 are given by $D_{self} = \frac{1}{6}k_{cage}a^2$ where $k_{cage} = 2k(S_{II} \rightarrow W)$ and $a \cong 11$ Å is the cage-to-cage length, as explained in our recent theoretical studies of benzene diffusion in Na-Y.[4,6] Figure 15 also indicates that the calculated diffusion coefficients are virtually insensitive to particular Na(II) distributions. As such, our calculations suggest that diffusion coefficients alone cannot distinguish between cage and cell cation distributions.

Underlying these diffusion coefficients are mean square displacements which may contain more information. Figure 16 shows benzene mean square displacements in Na-Y at $T=300$ K for Si:Al=3.0, 3.8 and 4.8. The Si:Al ratios 3.0 and 3.8 use cage disorder giving two and one Na(II) per supercage, respectively, while Si:Al=4.8 gives one Na(II) per unit cell, thus eliminating cation disorder. The only curious aspect in Fig. 16 is the sizable y-intercept for Si:Al =4.8, suggesting rapid diffusion at short times in this system.

To pursue this, we repeated the KMC calculation for Si:Al=4.8 using logarithmic binning to resolve short time dynamics as discussed in Sec. III B and Ref. 6. The log–log mean square displacement plot in Fig. 17 shows KMC data from two long runs (thin lines), and a smoothed version of the longer KMC run (thick line) portraying the converged mean square displacement. In linear regions of such a log–log plot, unit slope indicates normal diffusion with the y-intercept giving $\log_{10}(6D_{self})$. Figure 17 shows an early diffusive regime where benzene jumps rapidly among supercages containing no Na(II) ions, eventually becoming trapped at the lone S_{II} site. The early diffusive regime is analogous to benzene mobility in siliceous-Y,[11] although the rapid cage-to-cage hopping mechanism in our model is not specifically tailored for that system.[46] The trap duration is the mean residence time in the supercage containing Na(II), and the plateau $\langle R^2(t)\rangle$ value is the y-intercept in Fig. 16. Normal diffusion ensues for $t > \tau_{trap}$ giving the mean square displacement in Fig. 16 and the diffusion coefficient in Fig. 15. The results in Fig. 17 indicate that mean square displacements, while providing diffusion coefficients, can contain other interesting information as well.

To determine whether measuring mean square displacements can probe cation distributions in Na-Y, we show in Fig. 18 log–log benzene mean square displacement plots for Si:Al=3.0 and 3.8 comparing cage and cell disorder. These results contain interesting information about rapid and sluggish diffusion as was found in Fig. 17, but also demonstrate qualitative insensitivity to particular Na(II) occupancy patterns. Our results therefore suggest that diffusion measurements cannot be used to infer cation distributions in Na-Y.

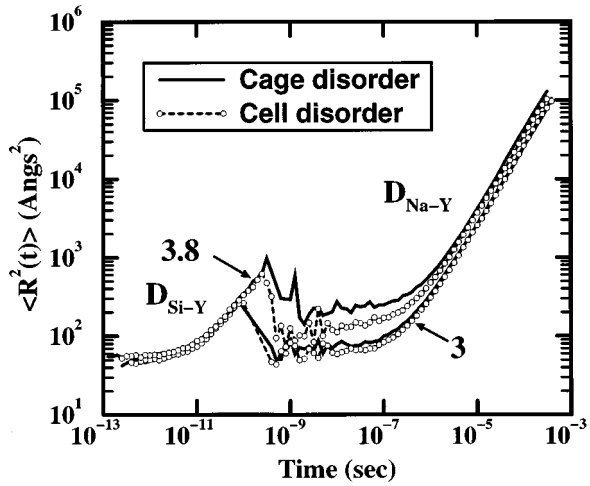

FIG. 18. The same as Fig. 17, except with Si:Al=3.0 and 3.8 comparing cage and cell disorder, suggesting that mean square displacements are qualitatively insensitive to different cation distributions in Na-Y.

V. CONCLUDING REMARKS

We have performed kinetic Monte Carlo (KMC) simulations of benzene mobility in Na-Y with various Na(II) cation occupancies. We evaluate a second-order orientational correlation function with KMC to quantify rates of benzene orientational randomization (BOR). Full Na(II) occupancy gives BOR rates controlled by intracage motion, whereas half Na(II) occupancy gives BOR rates sensitive to both intracage and intercage motion, but insensitive to particular Na(II) spatial patterns. Alternatively, BOR with one quarter Na(II) occupancy demonstrates *qualitative sensitivity* to different Na(II) spatial patterns.

In order to compare the information obtained from BOR in Na-Y with that available from benzene diffusion in Na-Y, we have used KMC to calculate benzene mean square displacements and diffusion coefficients for various temperatures, Na(II) occupancies and Na(II) spatial patterns. The calculated diffusion coefficients vary weakly with decreasing Na(II) occupancy until ca. one Na(II) per supercage. Diffusion coefficients and mean square displacements reveal no information about intracage motion, and are insensitive to different spatial patterns of Na(II) cations.

Our computational results thus suggest that measuring orientational randomization in zeolites can provide important information complementary to that obtained from diffusion measurements. Indeed, we predict that using two-dimensional exchange NMR to measure benzene's orientational correlation function in Ca-Y with half Ca(II) occupancy can simultaneously reveal intracage hopping rates and diffusion coefficients. This would provide an important link between the disparate length scales probed by NMR relaxation and pulsed field gradient (PFG) NMR. We further predict that performing such a measurement in Ca-Y with one quarter Ca(II) occupancy can provide unprecedented information about disordered cation distributions. Chmelka and co-workers are particularly well poised to undertake such experiments.[24,25]

Several aspects of our model can be improved in order to strengthen our predictions. We plan to calculate dynamically exact hopping rate coefficients to remove assumptions regarding Arrhenius temperature dependence. We also plan to correct these hopping rate coefficients for inhomogeneities introduced by cation vacancies, and will incorporate finite benzene loadings to determine effects from guest–guest interactions. Finally, we plan to extend these calculations to other host–guest systems to determine how widely applicable our conclusions remain. Nevertheless, our results for benzene in cation-containing faujasites are sufficiently remarkable that they deserve attention at this initial level of theory.

ACKNOWLEDGMENTS

We thank Dr. D. J. Schaefer, Professor B. F. Chmekla and Professor K. Schmidt-Rohr for enlightening discussions regarding solid state NMR. S. M. A. acknowledges support from the National Science Foundation (NSF) under Grants No. CHE-9403159 and No. CHE-9625735, and from MSI for generously providing visualization software. H. I. M. acknowledges the NSF and the Office of Naval Research for funding. This work made use of UCSB-MRL Central Facilities supported by the NSF under Award No. DMR-9123048.

[1] J. Kärger and D. M. Ruthven, *Diffusion in Zeolites and Other Microporous Solids* (Wiley, New York, 1992).
[2] J. Weitkamp, in *Catalysis and Adsorption by Zeolites*, edited by G. Olhmann, J. C. Vedrine, and P. A. Jacobs (Elsevier, Amsterdam, 1991), p. 21.
[3] J. M. Newsam, ''Zeolites,'' in *Solid State Chemistry: Compounds*, edited by A. K. Cheetham and P. Day (Oxford University Press, Oxford, 1992), pp. 234–280.
[4] S. M. Auerbach, N. J. Henson, A. K. Cheetham, and H. I. Metiu, J. Phys. Chem. **99**, 10600 (1995).
[5] S. M. Auerbach, L. M. Bull, N. J. Henson, H. I. Metiu, and A. K. Cheetham, J. Phys. Chem. **100**, 5923 (1996).
[6] S. M. Auerbach and H. I. Metiu, J. Chem. Phys. **105**, 3753 (1996).
[7] A. Germanus, J. Kärger, H. Pfeifer, N. N. Samulevic, and S. P. Zdanov, Zeolites **5**, 91 (1985).
[8] B. Boddenberg and R. Burmeister, Zeolites **8**, 488 (1988).
[9] B. Boddenberg and B. Beerwerth, J. Phys. Chem. **93**, 1440 (1989).
[10] R. Burmeister, H. Schwarz, and B. Boddenberg, Ber. Bunsenges. Phys. Chem. **93**, 1309 (1989).
[11] L. M. Bull, N. J. Henson, A. K. Cheetham, J. M. Newsam, and S. J. Heyes, J. Phys. Chem. **97**, 11776 (1993).
[12] K. A. Fichthorn and W. H. Weinberg, J. Chem. Phys. **95**, 1090 (1991).
[13] R. L. June, A. T. Bell, and D. N. Theodorou, J. Phys. Chem. **95**, 8866 (1991).
[14] H. I. Metiu, Y. T. Lu, and Z. Y. Zhang, Science **255**, 1088 (1992).
[15] H. W. Spiess, *NMR Basic Principles and Progress* (Springer-Verlag, Berlin, 1978), Vol. 15.
[16] D. A. Torchia and A. Szabo, J. Magn. Reson. **49**, 107 (1982).
[17] K. Schmidt-Rohr and H. W. Spiess, *Multidimensional Solid-State NMR and Polymers* (Academic Press, London, 1994).
[18] V. Voss and B. Boddenberg, Surf. Sci. **298**, 241 (1993).
[19] A. N. Fitch, H. Jobic, and A. Renouprez, J. Phys. Chem. **90**, 1311 (1986).
[20] Here we have assumed an axially symmetric coupling tensor, which is exact for C–H bonds and an excellent approximation for C–D bonds.
[21] M. E. Rose, *Elementary Theory of Angular Momentum* (Wiley, New York, 1967).
[22] H. Klein, H. Fuess, and G. Schrimpf, J. Phys. Chem. **100**, 11101 (1996).
[23] J. A. Sousa Goncalves, R. L. Portsmouth, P. Alexander, and L. F. Gladden, J. Phys. Chem. **99**, 3317 (1995).
[24] M. Wilhelm, A. Firouzi, D. E. Favre, L. M. Bull, D. J. Schaefer, and B. F. Chmelka, J. Am. Chem. Soc. **117**, 2923 (1995).
[25] D. J. Schaefer, D. E. Favre, and B. F. Chmelka (in preparation).
[26] Off-diagonal intensity can also arise from, e.g., dipole–dipole interactions generating magnetization transfer between different resonance frequencies without molecular jumping, i.e., spin diffusion. For an experimental discussion of this effect, see Ref. 25.
[27] P. Demontis, S. Yashonath, and M. L. Klein, J. Phys. Chem. **93**, 5016 (1989).
[28] L. Uytterhöven, D. Dompas, and W. J. Mortier, J. Chem. Soc. Faraday Trans. **88**, 2753 (1992).
[29] H. Klein, C. Kirschhock, and H. Fuess, J. Phys. Chem. **98**, 12345 (1994).
[30] P. J. O'Malley and C. J. Braithwaite, Zeolites **15**, 198 (1995).
[31] M. M. Eddy, Ph.D. thesis, Oxford University, 1985.
[32] R. Gomer, Rep. Prog. Phys. **53**, 917 (1990).
[33] D. A. Dougherty, Science **271**, 163 (1996).
[34] P. Maksym, Semicond. Sci. Technol. **3**, 594 (1988).
[35] M. Alonso and E. J. Finn, *Fundamental University Physics: Fields and Waves*, 2nd ed. (Addison-Wesley, Reading MA, 1983), Vol. 2.
[36] This analysis ignores charge–quadrupolar anisotropy, and as such provides an orientationally averaged error estimate.
[37] T. Ohgushi and S. Sato, J. Sol. State Chem. **87**, 95 (1990).
[38] T. Ohgushi and S. Kataoka, J. Colloid. Interface Sci. **148**, 148 (1992).
[39] T. Ohgushi and Y. Kawanabe, Zeolites **14**, 356 (1994).
[40] J. Kärger (private communication).
[41] J. Kärger and D. M. Ruthven, J. Chem. Soc., Faraday Trans. I **77**, 1485 (1981).

[42] G. Vitale, L. M Bull, R. E. Morris, A. K. Cheetham, B. H. Toby, C. G. Coe, and J. E. MacDougall, J. Phys. Chem. **99**, 16087 (1995).
[43] D. J. Schaefer, S. M. Auerbach, and B. F. Chmelka (in preparation).
[44] Rotational diffusion about benzene's six-fold axis and random librational motion of the six-fold axis contribute to BOR with one S_{II} site per supercage. These motions, however, give relatively limited BOR and have been ignored for simplicity.
[45] M. T. Melchior, D. E. W. Vaughan, and C. F. Pictroski, J. Phys. Chem. **99**, 6128 (1995).
[46] N. J. Henson, Ph.D. thesis, Oxford University, 1996.